PLOS | ONE

RESEARCH ARTICLE

Dose Optimization in TOF-PET/MR Compared to TOF-PET/CT

Marcelo A. Queiroz[1]*, Gaspar Delso[2], Scott Wollenweber[2], Timothy Deller[2], Konstantinos Zeimpekis[1], Martin Huellner[1,3], Felipe de Galiza Barbosa[1], Gustav von Schulthess[1], Patrick Veit-Haibach[1,3]

1 Department of Medical Imaging, Nuclear Medicine, University Hospital Zurich, Zurich, Switzerland, **2** GE Healthcare, Waukesha, Wisconsin, United States of America, **3** Department of Medical Imaging, Diagnostic and Interventional Radiology, University Hospital Zurich, Zurich, Switzerland

* marcelo.araujoqueiroz@gmail.com

Citation: Queiroz MA, Delso G, Wollenweber S, Deller T, Zeimpekis K, Huellner M, et al. (2015) Dose Optimization in TOF-PET/MR Compared to TOF-PET/CT. PLoS ONE 10(7): e0128842. doi:10.1371/journal.pone.0128842

Editor: Kewei Chen, Banner Alzheimer's Institute, UNITED STATES

Received: January 16, 2015

Accepted: April 30, 2015

Published: July 6, 2015

Data Availability Statement: All relevant data are within the paper.

Funding: This research project was supported by an institutional research grant from GE Healthcare. Co-authors Gaspar Delso, Scott D. Wollenweber and Timothy Deller are employed by GE Healthcare. GE Healthcare provided support in the form of salaries for authors GD, SDW and TD, but did not have any additional role in the study design, data collection and analysis, decision to publish, or preparation of the manuscript. The specific roles of these authors are articulated in the 'author contributions' section.

Abstract

Purpose

To evaluate the possible activity reduction in FDG-imaging in a Time-of-Flight (TOF) PET/MR, based on cross-evaluation of patient-based NECR (noise equivalent count rate) measurements in PET/CT, cross referencing with phantom-based NECR curves as well as initial evaluation of TOF-PET/MR with reduced activity.

Materials and Methods

A total of 75 consecutive patients were evaluated in this study. PET/CT imaging was performed on a PET/CT (time-of-flight (TOF) Discovery D 690 PET/CT). Initial PET/MR imaging was performed on a newly available simultaneous TOF-PET/MR (Signa PET/MR). An optimal NECR for diagnostic purposes was defined in clinical patients ($NECR_P$) in PET/CT. Subsequent optimal activity concentration at the acquisition time ($[A]_0$) and target NECR ($NECR_T$) were obtained. These data were used to predict the theoretical FDG activity requirement of the new TOF-PET/MR system. Twenty-five initial patients were acquired with (retrospectively reconstructed) different imaging times equivalent for different activities on the simultaneous PET/MR for the evaluation of clinically realistic FDG-activities.

Results

The obtained values for $NECR_P$, $[A]_0$ and $NECR_T$ were 114.6 (± 14.2) kcps (Kilocounts per second), 4.0 (± 0.7) kBq/mL and 45 kcps, respectively. Evaluating the $NECR_T$ together with the phantom curve of the TOF-PET/MR device, the theoretical optimal activity concentration was found to be approximately 1.3 kBq/mL, which represents 35% of the activity concentration required by the TOF-PET/CT. Initial evaluation on patients in the simultaneous TOF-PET/MR shows clinically realistic activities of 1.8 kBq/mL, which represent 44% of the required activity.

Competing Interests: This research project was supported by an institutional research grant from GE Healthcare. Co-authors Gaspar Delso, Scott D. Wollenweber and Timothy Deller are employed by GE Healthcare. PVH received IIS Grants from Bayer Healthcare, Siemens Medical Solutions, Roche Pharma and GE Healthcare and speaker fees from GE Healthcare. GvS is a grant recipient from GE Healthcare and received speaker fees from GE Healthcare. There are no patents, products in development or marketed products to declare. This does not alter the authors' adherence to all the PLOS ONE policies on sharing data and materials.

Conclusion

The new TOF-PET/MR device requires significantly less activity to generate PET-images with good-to-excellent image quality, due to improvements in detector geometry and detector technologies. The theoretically achievable dose reduction accounts for up to 65% but cannot be fully translated into clinical routine based on the coils within the FOV and MR-sequences applied at the same time. The clinically realistic reduction in activity is slightly more than 50%. Further studies in a larger number of patients are needed to confirm our findings.

Introduction

Positron emission tomography/magnetic resonance (PET/MR) using 18-Fluoro-deoxyglucose (FDG) opens potentially new perspectives in the field of clinical molecular imaging. Combining the high soft tissue contrast of MR, functional image procedures of MR and the molecular ability of PET may improve the anatomical correlation and provide more clinically relevant information [1]. As a new imaging modality, it is hoped that PET/MR shows some significant advantages over PET/Computed tomography (CT) e.g. in head and neck cancer evaluation [2,3] or liver metastases detection [4]. Besides the potential of improved lesion characterisation, one expected benefit is the reduction of radiation exposure by omitting the CT–based dose and also reducing the FDG- activity requirement[5]. Such a reduction in activity in the PET-component of the evaluated TOF-PET/MR system can be achieved e.g. with a combination of silicon-based detector technology and larger solid angle coverage [6,7].

The noise-equivalent count rate (NECR) represents an objective measurement of PET-system performance that reflects the ratio of true events to the overall detected events, which include randoms and scatters [8]. It is calculated following the National Electrical Manufacturers Association (NEMA) recommendations, using a 20-cm-diameter and 70-cm-long cylinder that is assumed to provide a reasonable characterization of whole-body image quality [9].

The noise equivalent count rate is the standard metric for PET scanner performance provided by the manufacturers and determined as part of acceptance testing for new equipment [10].

However, obtaining the NECR values from phantoms does not entirely reflect clinical routine behavior in patients since this measurement simply does not account for variations in the fractions of the scatter and random events that are internal to the patient [11].

In a pre-evaluation to this presented study, it was shown that NECR measured in patients can predict clinically perceived image quality in PET-imaging and a corresponding FDG-activity threshold above which the acquired PET images have good-to-excellent perceived quality in more than 90% of patients [12].

Using these data as the basis of the present study, we use the NECR measured in patients in PET/CT to predict the theoretically achievable FDG-activities in a new whole-body TOF-PET/MR, based on the NECR curves measured in a standard NEMA phantom.

The aim of the study was (1) to investigate the amount of *theoretically* possible dose reduction in a new TOF-PET/MR compared to standard TOF-PET/CT by comparison of NECR-measurements in patients (in PET/CT) and NECR measured in phantoms (PET/MR) and (2) to evaluate the *clinically realistic* reduction in activity in PET/MR by evaluation of different (retrospectively reconstructed) imaging times which are equivalent to different FDG-activities.

Materials and Methods

Patient population

A total of 75 consecutive patients (81 exams) were evaluated retrospectively. All patients were referred for a clinical FDG-PET/CT from January to December/2012 and underwent a PET/CT-MR using a tri-modality setup. Based on the retrospective nature of the study, no formal institutional ethics committee approval was needed and a waiver was provided.

Exclusion criteria applied were uncontrolled glucose levels and patients who did not fast for a minimum of 4 hours prior to the examination, unwillingness to undergo the additional MR examination, claustrophobia, MR-incompatible medical devices (e.g. cardiac pacemaker, insulin pump, neurostimulator, cochlear implant). Another exclusion criterion was presence of artefacts in at least one bed-position, which made clinical reading not applicable. Parts of the evaluated patient population were also evaluated within the context of another study which is currently under review as well.

PET/CT imaging

PET/CT imaging was performed on a PET/CT-MR setup including a time-of-flight Discovery 690 PET/CT and a Discovery 750w 3T MR (both GE Healthcare, Waukesha, WI).

PET/CT was performed according to the EANM procedure guidelines for tumour PET imaging [13]. Patients fasted for at least 4 hours prior to injection of ^{18}F-fluorodeoxyglucose (FDG). The mean FDG injected activity was 311.7 MBq (SD = 21.3 MBq, range 231.1–373.4 MBq). The mean FDG injected activity/body weight was 4.3 MBq/kg (SD = 0.9 MBq/kg, range 2.6–6.6 MBq/kg).

Unenhanced low-dose CT and PET emission data were acquired from the mid-thigh to the vertex of the skull. CT data were acquired in shallow-breathing with dose modulation between 15–80 mA, 120 kVp and a pitch of 0.984:1, reconstructed to images of 0.98 mm transverse pixel size and 3.75 mm slice thickness. PET data was acquired in 3D time-of-flight mode with scan duration of 2 min per bed position, an axial FOV of 153 mm and a 23% overlap of bed positions, resulting in a total PET acquisition time ranging from 16 to 20 minutes. The emission data were corrected for randoms, dead time, scatter and attenuation and iteratively reconstructed (OSEM, 3 iterations, 18 subsets)[3].

Image processing and analysis

The acquired PET and CT images were transmitted to a dedicated review workstation (Advantage Workstation, GE Healthcare), which enables the review of the PET and CT images side by side or in fused/overlay mode (PET/CT).

In a first step, all data were automatically analysed using Matlab (MathWorks, Natick, MA, USA) to estimate the noise-equivalent count rate (NECR) versus activity concentration in a similar manner to the National Electrical Manufacturers Association (NEMA) analysis, including scatter or attenuation correction methods applied to patient data and how scatter and randoms were estimated, based on previous publications [11,14–17]. This measurement is essentially the same usually performed on phantom data, but the required data (the number of true, scattered and random counts) are estimations either provided by the scanner software or automatically extracted from the reconstructed image. Methods how to evaluate NECR measurements in patients have been described before by different authors [8,11,15]. To highlight the fact that these NECR values were measured on patient data, we indicate this as $NECR_P$.

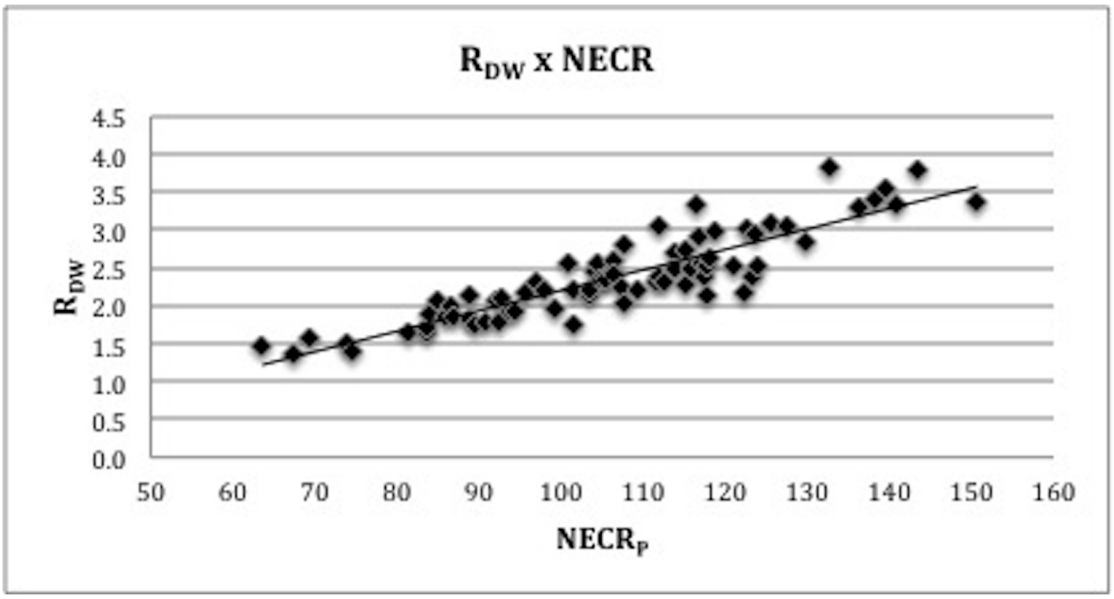

Fig 1. Relation between R_{DW} and R_{BMI} and clinical NECR measured in patients ($NECR_P$).

doi:10.1371/journal.pone.0128842.g001

In a second step, all the PET/CT exams were read by a board-certified nuclear medicine physician / radiologist and by a radiologist with substantial experience in PET/CT image reading.

One subjective score was defined to evaluate image quality. The *IQ local score* (IQ_L) was a three-point scale assigned to each bed position in axial plane in all patients (n = 655 bed positions), where 1 means poor, 2 means good and 3 means excellent IQ. In general, smoothness and sharpness of the images have been considered for the evaluation. The liver homogeneity and graininess and the contrast between different structures that accumulate different levels of tracer, like the lung and chest wall, were analysed.

Patient data were analysed concerning overall weight, body mass index (BMI) and FDG-activity at the start of acquisition (D_{Acq}). One additional parameter was defined for each patient: the ratio between D_{Acq} and patient weight (R_{DW}).

The R_{DW} threshold was determined, above which the resulting image quality was at least "good" ($IQ_L > 2$) in more than 90% of patients. The rationale for choosing R_{DW} as the threshold parameter is that this measurement is routinely used to calculate patient's dose, according to EANM guidelines, making it more reproducible. Using the R_{DW} threshold, the optimal $NECR_P$ for diagnostic purposes was defined based on the R_{DW} x $NECR_P$ curve (Fig 1).

The $NECR_P$ was then cross-referenced in the graphic $NECR_P$ x Activity concentration (Fig 2) in order to get the corresponding optimal activity concentration at the acquisition time ($[A]_0$). By obtaining this value, it is now possible to establish the relation between patient-based and phantom-based count-rate measurements. Applying the calculated $[A]_0$ value on the NEMA phantom curve of the GE Discovery D690 (Fig 3) that was used in these acquisitions, the target NECR ($NECR_T$) was obtained. Notice that this image quality target value is independent of the PET system used.

Using this $NECR_T$, it is therefore possible to estimate, for any PET system, the activity concentration required to obtain the desired image quality (e. g. good-to-excellent") in a given percentage of patients ($[A]_N$), by cross-evaluation with the NECR curves of the system compared.

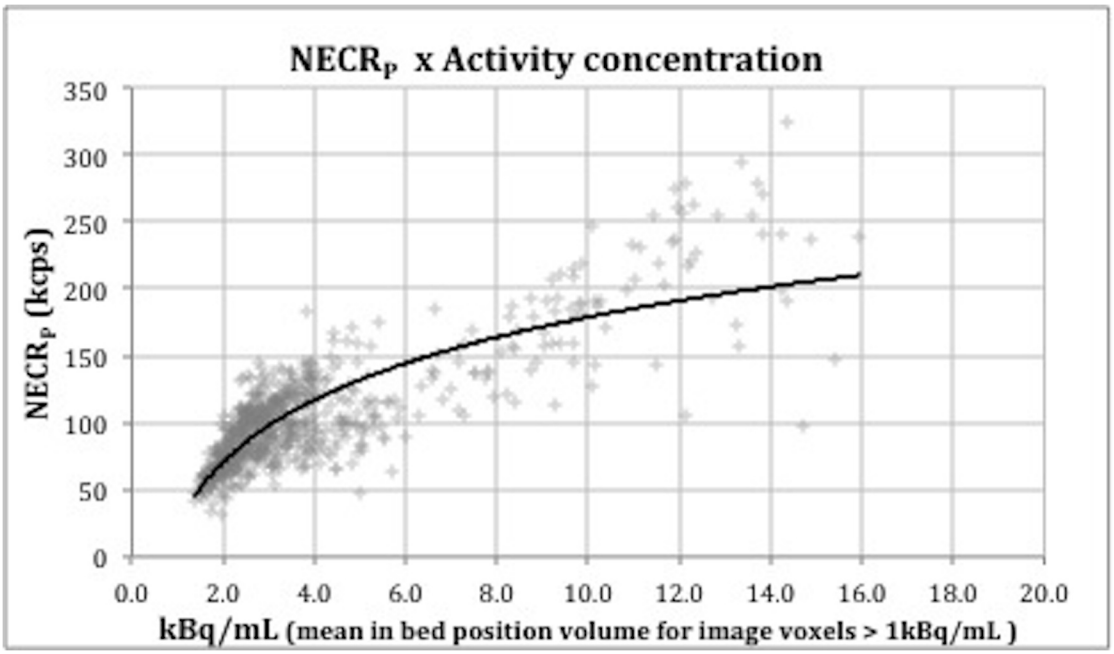

Fig 2. Relation between NECR measured in patients and activity concentration.

doi:10.1371/journal.pone.0128842.g002

In a pre-evaluation a threshold in which 90% of cases were rated with "good to excellent" image quality was defined [12].

In the presented study, this procedure was performed for the particular case of a new whole-body TOF-PET/MR device in order to predict the injected FDG- activity needed to

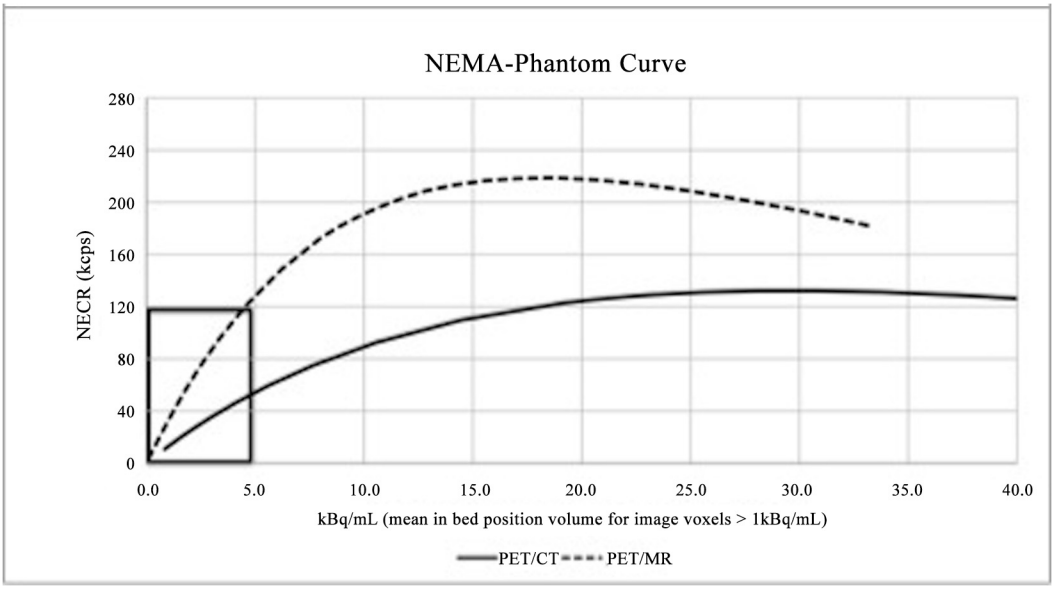

Fig 3. The NEMA phantom curve of the TOF-PET/CT (continuous) and TOF-PET/MR (dashed), provided by its manufacturer. See enlarged image of the clinically relevant area (black box) in Fig 4.

doi:10.1371/journal.pone.0128842.g003

provide good-to-excellent images, which is expected to be significant lower. The GE Signa PET/MR is a whole-body scanner combining a 3T wide-bore MR system with a 25 cm PET detector ring based on SiPM technology and mounted on a customized radiofrequency coil.

Furthermore to transfer our results not only technically but also clinically, the first 25 patients on the new simultaneous TOF-PET/MR were evaluated as well. For this purpose, (acquired 2 min/bed in PET/CT and 4 min/bed in simultaneous TOF-PET/MR) patient-data was reconstructed retrospectively to expose both systems to the same amount of *emitted* counts. Reconstructed acquisition times were adjusted for tracer decay between the acquisitions.

The acquisition times were reconstructed to be similar by unlisting the list mode data and creating similar sinograms to be compared for each acquisition time. This way, the two resulting sinograms are representing an equivalent of the same injected ^{18}F-FDG acitivity. After reducing PET/MR acquisition times to match the PET/CT decay integral, the average was 196 ± 25 seconds/bed.

Our next step was to reduce both, PET/CT and PET/MR acquisition times in pre-defined steps to evaluate at which time point the PET/CT and/or the PET/MR image were considered not "good to excellent" anymore. For these whole body scans, we un-listed the emission data for 120, 100, 80, 60, 40 and 30 seconds/bed for PET/CT; the corresponding equivalent times for PET/MR were 206, 170, 134, 98, 68, 53 ± 25 seconds/bed. By defining this threshold, and again applying the calculated value on the NEMA phantom curve of the simultaneous PET/MR system, it is possible to extrapolate not only a theoretical "technical" threshold for activity reduction but also a clinically validated threshold.

Statistical Analysis

All statistical tests were performed using SPSS Statistics Version 21 (IBM, Armonk, NY, USA). *P*-values < 0.05 were considered statistically significant. Pearson's correlation analysis was performed to evaluate the relation between NECR, and R_{DW}.

Results

The R_{DW} was significantly correlated with $NECR_P$ ($r = 0.89$, p-value < 0.01), as presented on Fig 1. The threshold at scan time calculated for R_{DW} was 2.6 MBq/kg.

The obtained values for $NECR_P$, $[A]_0$ and $NECR_T$ were 114.6 (± 14.2) kcps, 4.0 (± 0.7) kBq/mL and 45 kcps, respectively. Cross-referencing this $NECR_T$ to the phantom curve of the new TOF-PET/MR system (Fig 3), the corresponding activity concentration at scan time was found to be approximately 1.4 kBq/mL. At this activity concentration, 90% of images would be rated with "good to excellent" image quality.

Thus, the theoretical activity concentration required by the new TOF- PET/MR is 35% of the activity concentration required by the TOF- PET/CT. The corresponding ideal activity threshold at the injection time is 1.3 MBq/kg.

With the same method it is possible to calculate and find any required clinical image quality threshold as well as the required threshold for the injected activity for any system for which the NECR curve is available. Considering 3.8 MBq/kg as the optimal threshold at injection time for the compared TOF-PET/CT, which requires an activity concentration of 4.0 kBq/mL, the optimal threshold could be calculated with $T_O = 0.95 \times [A]_N$, where the $[A]_N$ is the activity concentration value for which the corresponding NECR is 45 kcps in the NECR curve.

Since these values are representing the theoretically possible reduction in injected activity, the evaluation on the simultaneously acquired PET/MRI showed slightly different results.

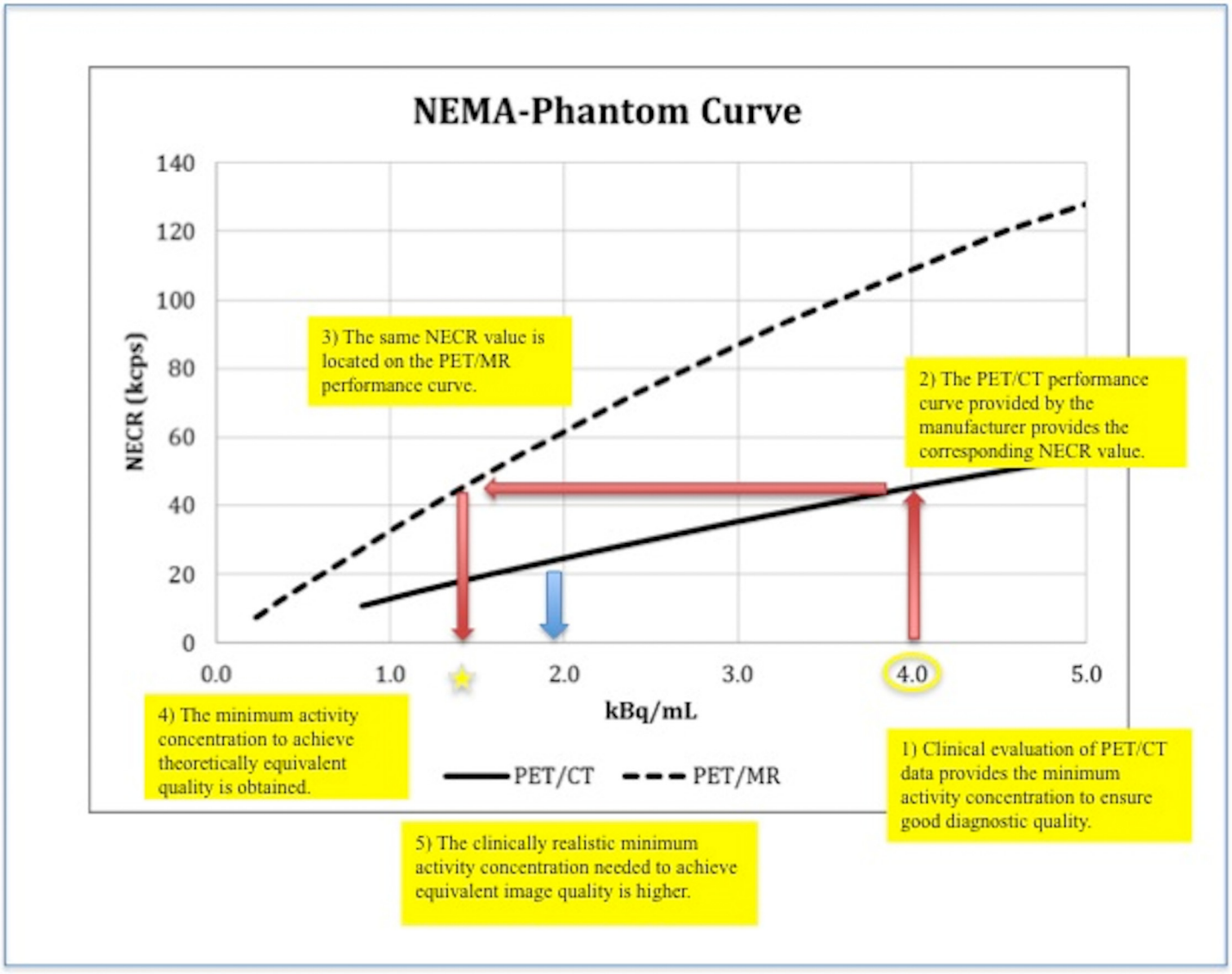

Fig 4. Evaluation and transfer steps from activities in PET/CT (1) to theoretically (2,3) achievable reduction in injected activity in TOF-PET/MR (4) and clinically realistically activities in TOF-PET/MR (5—blue arrow).

doi:10.1371/journal.pone.0128842.g004

Here, on average the PET/MR image was rated not "good to excellent" anymore at a time point equivalent to 1.8 kBq/mL which represents 44% of the initially required activity (Fig 4).

Discussion

This study is an extension of a previous study about clinical image quality perception and corresponding NECR measurements in PET systems. The results of this pre-evaluation indicated that findings based on the $NECR_P$ metric could be rescaled and applied for different PET systems [8,11,15,18]. Other groups have evaluated methods about NECR measurements in patients and corresponding image quality as well [8,19,20]. In the presented study, to the best of our knowledge, we are the first to present the extrapolation of clinically evaluated image quality and corresponding NECR measurements in patients from PET/CT to a new TOF-PET/

MR (SIGNA PET/MR, GE Healthcare, Waukesha, MI, USA). Our results show that with this new system, a theoretical reduction in injected activity down to nearly one third of ^{18}F-FDG, and a clinically realistic reduction of slightly more than 50% in FDG-activity compared to a TOF-PET/CT is possible.

Much effort has been put into optimization of the injected FDG-activity and maintaining image quality at the same time. Ideally, FDG-activity should be kept as low as possible considering the cost of the tracer and the radiation exposure for the patient and staff [21]. Patient morphology, the time acquisition per bed position and the used PET reconstruction (e.g. 2D vs. 3D, time of flight) are some of the parameters that have been shown to influence the FDG-dosing requirements [11,16,21].

However, regardless all of these parameters, the performance of every PET scanner is intrinsically (and non-linearly) dependent on the amount of injected activity. Although there is a debate on how to derive NECR values, the measurements following the NEMA protocol represent one of the most accepted and widely used way of showing the relation between the activity and acquired data quality. The controversial issue concerning the use of NECR is the difficulty to extrapolate the phantom-based measurements to patient acquisitions, since the response in humans can be quite variable [11]. The use of NECR nevertheless appears as a potential tool to standardize the FDG activity needed to get images in diagnostic quality. One possibility is to measure the NECR directly in clinical patients, which has already been done in other studies [8,11].

Recently, McDermott et. al have shown that the noise equivalent counts per axial length was also an effective and objective indicator of patient image quality, being able to discriminate images of good/excellent quality from those of poorer image quality with higher degree of accuracy than noise equivalent count density and liver signal to noise ratio [22].

Another challenge of correlating the NECR measured in patients to the visually perceived PET-image quality assessed by imaging specialists. Previous studies have compared the NECR phantom-based to visual image quality [17,19] or NECR measured in patients to signal-to-noise as a parameter of image quality [8,11].

As an initial step, our study compared the NECR measured in patients and visual image quality assessed by nuclear medicine physicians/radiologists, favouring the clinical reliability of our findings compared to other available studies that were not assessed by imaging specialists.

In a second step, the newly available TOF-PET/MR has been evaluated using the NEMA recommendations. A NECR curve (phantom based) has been created and was used to estimate the theoretically required activity concentration in order to achieve again good-to-excellent images. In the last step these results were then evaluated and transferred to the simultaneously acquired PET/MR images to evaluate the clinically realistic reduction in injected activity.

Our findings suggest that the optimal activity concentration required in the PET/MR is 35% (a reduction of 65%) of the activity concentration required by the comparatively used TOF-PET/CT. There are several technical reasons and explanations for this.

Delso et. al have already suggested that the integrated PET/MR features could require lower activities[5]. For a non-TOF whole-Body PET/MR used by Delso et al., a longer axial FOV and reduced detector ring diameter lead to higher count rates and an increased sensitivity, both in stand-alone operation and with simultaneous MR image acquisition. Thus, such a PET/MR system reaches its saturation and dead-time points with lower activities[5].

The evaluated TOF-PET/MR system has an increased axial field of view (FOV) compared to the TOF-PET/CT, too. Thus, the increased axial FOV increases sensitivity at the scanner center in a d^2 (axial field of view) relationship. For example, going from 15 to 25cm axial FOV leads to $(25/15)^2$, which is a 2.78 factor improvement.

Another feature of the evaluated system scanner is the diameter compared to standard PET/CT, which also provides an approximately linear gain in sensitivity. For example here, going from 810 mm to 622 mm diameter leads to (810/622) a factor of 1.3 of improvement. The evaluated PET/MR has a detector face-to-face diameter of 62 cm and an axial FOV of 25 cm in PET.

Concerning detector configuration, the new PET system employs five rings of 112 detector blocks where the scintillator crystals are coupled to 1 x 3 arrays of SiPM devices. The SiPM itself has several advantages compared with conventional detector materials, e.g. timing resolution, gain and corresponding noise [23,24].

The PET detectors modules are mounted on the outside of a novel radiofrequency (RF) body coil that provides additional space to accommodate the PET detector ring with a 60 cm patient bore. This design also reduces the amount of PET-attenuating material in the PET field of view, contributing in part to the reduced activity requirements. The use of scatter recovery techniques additionally supports this advantage as well [25].

A recent study has evaluated the advantage of the implementation of such recovery procedures by using the inter-block Compton scatter on TOF-PET scanners. It was found that this setup is expected to result in an overall scanner sensitivity improvement of up to 20% without significant processing overhead [25].

Summing up all these newly embedded technologies in the evaluated TOF-PET/MR, the analysed system has the potential to require significantly less activity while preserving diagnostic image quality.

However, there are also several reasons to consider why those improvements in dosage are not fully translated into clinical routine. To make full use of the system's capabilities, the full field-of-view has to be used to achieve the full sensitivity. This is obviously not possible for brain imaging where the "natural" field-of-view is shorter.

Furthermore, one has to account for the MR-coils within the PET-FOV, which causes a decrease in counts as well. This is especially important for brain imaging, because the head/neck coils are a fully surrounding cage, while surface coils for body imaging are made of less material and are more flexible [26–29]. Thus, in cases of brain imaging, one might loose up to 15–20% of sensitivity in the center of the image based on the head and neck coil. Surface coils however, account for a smaller amount of sensitivity loss [30].

Lastly, the execution of MR-sequences are known to decrease the performance of PET-systems, too, however, largely not clinically significant ($< 5\%$) [31]. Summing up these additional considerations, an activity reduction of up to 65% (or using just 35% of the activity compared to current TOF-PET/CT) is a theoretical number, but clinical reality as initially evaluated here also shows roughly a reduction in injected activity of $> 50\%$.

One limitation is certainly that we only evaluated the first initial patients on the simultaneous PET/MR to test the clinical transferability of our results.

Furthermore, clinical image perception is always prone to a certain extent of subjectivity of the readers; clinical image perception in PET/MRI might be different compared to PET/CT.

Conclusion

The new TOF-PET/MR device requires significantly less activity to generate PET-images with good-to-excellent image quality, due to improvements in detector geometry and detector technologies. The theoretical achievable reduction of ^{18}F-FDG acitivity was proven based on cross-evaluation of clinical images quality in PET/CT and phantom based NECR measurements in TOF-PET/MRI. Further studies in a larger number of patients are needed to confirm our findings.

Author Contributions

Conceived and designed the experiments: MAQ GD SW TD KZ MH FGB GvS PVH. Performed the experiments: MAQ GD SW. Analyzed the data: MAQ GD SW KZ MH FGB PVH. Contributed reagents/materials/analysis tools: MAQ GD SW TD KZ MH FGB GvS PVH. Wrote the paper: MAQ GD SW TD KZ MH FGB GvS PVH.

References

1. Kalemis A, Delattre BMa, Heinzer S. Sequential whole-body PET/MR scanner: concept, clinical use, and optimisation after two years in the clinic. The manufacturer's perspective. MAGMA 26: 5–23. doi: 10.1007/s10334-012-0330-y PMID: 22868642
2. Kuhn FP, Hüllner M, Mader CE, Kastrinidis N, Huber GF, von Schulthess, et al. Contrast-enhanced PET/MR imaging versus contrast-enhanced PET/CT in head and neck cancer: how much MR information is needed? J Nucl Med 55: 551–558. doi: 10.2967/jnumed.113.125443 PMID: 24491410
3. Queiroz MA, Hüllner M, Kuhn F, Huber G, Meerwein C, Kollias S, et al. PET/MRI and PET/CT in follow-up of head and neck cancer patients. Eur J Nucl Med Mol Imaging 41: 1066–1075. doi: 10.1007/s00259-014-2707-9 PMID: 24577950
4. Reiner CS, Stolzmann P, Husmann L, Burger IA, Hüllner MW, Schaefer NG, et al. Protocol requirements and diagnostic value of PET/MR imaging for liver metastasis detection. Eur J Nucl Med Mol Imaging 41: 649–658. doi: 10.1007/s00259-013-2654-x PMID: 24346415
5. Delso G, Fürst S, Jakoby B, Ladebeck R, Ganter C, Nekolla SG, et al. Performance measurements of the Siemens mMR integrated whole-body PET/MR scanner. J Nucl Med 52: 1914–1922. doi: 10.2967/jnumed.111.092726 PMID: 22080447
6. Delso G, Martinez M-J, Torres I, Ladebeck R, Michel C, Nekolla SG, et al. Monte Carlo simulations of the count rate performance of a clinical whole-body MR/PET scanner. Med Phys 36: 4126–4135. PMID: 19810486
7. Akamatsu G, Mitsumoto K, Ishikawa K, Taniguchi T, Ohya N, Baba S, et al. Benefits of point-spread function and time of flight for PET/CT image quality in relation to the body mass index and injected dose. Clin Nucl Med 38: 407–412. doi: 10.1097/RLU.0b013e31828da3bd PMID: 23603585
8. Chang T, Chang G, Kohlmyer S, Clark JW, Rohren E, Mawlawi OR, et al. Effects of injected dose, BMI and scanner type on NECR and image noise in PET imaging. Phys Med Biol 56: 5275–5285. doi: 10.1088/0031-9155/56/16/013 PMID: 21791730
9. Daube-Witherspoon ME, Karp JS, Casey ME, DiFilippo FP, Hines H, Muehllehner G, et al. PET performance measurements using the NEMA NU 2–2001 standard. J Nucl Med 43: 1398–1409. PMID: 12368380
10. Badawi RD, Dahlbom M. NEC: some coincidences are more equivalent than others. J Nucl Med 46: 1767–1768. PMID: 16269587
11. Watson CC, Casey ME, Bendriem B, Carney JP, Townsend DW, Eberl S, et al. Optimizing injected dose in clinical PET by accurately modeling the counting-rate response functions specific to individual patient scans. J Nucl Med 46: 1825–1834. PMID: 16269596
12. Queiroz M, Wollenweber SD, von Schulthess G, Delso G, Veit-Haibach P. Clinical image quality perception and corresponding NECR measurements in PET. EJNMMI Phys 1: 1–13.
13. Boellaard R, O'Doherty MJ, Weber W a, Mottaghy FM, Lonsdale MN, et al. FDG PET and PET/CT: EANM procedure guidelines for tumour PET imaging: version 1.0. Eur J Nucl Med Mol Imaging 37: 181–200. doi: 10.1007/s00259-009-1297-4 PMID: 19915839
14. Strother SC, Casey ME, Hoffman EJ. Measuring PET scanner sensitivity: relating countrates to image signal-to-noise ratios using noise equivalents counts. IEEE Trans Nucl Sci 37: 783–788.
15. Walker MD, Matthews JC, Asselin M-C, Saleem A, Dickinson C, Charnley N, et al. Optimization of the injected activity in dynamic 3D PET: a generalized approach using patient-specific NECs as demonstrated by a series of 15O-H2O scans. J Nucl Med 50: 1409–1417. doi: 10.2967/jnumed.109.062679 PMID: 19690021
16. Lartizien C, Comtat C, Kinahan PE, Ferreira N, Bendriem B, Trésbossen R, et al. Optimization of injected dose based on noise equivalent count rates for 2- and 3-dimensional whole-body PET. J Nucl Med 43: 1268–1278. PMID: 12215569
17. Danna M, Lecchi M, Bettinardi V, Gilardi M, Stearns C, Lucignani G, et al. Generation of the Acquisition-Specific NEC (AS-NEC) Curves to Optimize the Injected Dose in 3D 18F-FDG Whole Body PET Studies. IEEE Trans Nucl Sci 53: 86–92.

18. Groot E de, Post N, Boellaard R. Optimized dose regimen for whole-body FDG-PET imaging. EJNMMI Res 3:1–11. doi: 10.1186/2191-219X-3-1 PMID: 23281702

19. Mizuta T, Senda M, Okamura T, Kitamura K, Inaoka Y, Takahashi M, et al. NEC density and liver ROI S/N ratio for image quality control of whole-body FDG-PET scans: comparison with visual assessment. Mol imaging Biol 11: 480–486. doi: 10.1007/s11307-009-0214-3 PMID: 19330382

20. Chang T, Chang G, Clark JW, Diab RH, Rohren E, Mawlawi OR, et al. Reliability of predicting image signal-to-noise ratio using noise equivalent count rate in PET imaging. Med Phys 39: 5891–5900. doi: 10.1118/1.4750053 PMID: 23039628

21. Everaert H, Vanhove C, Lahoutte T, Muylle K, Caveliers V, Bossuyt A, et al. Optimal dose of 18F-FDG required for whole-body PET using an LSO PET camera. Eur J Nucl Med Mol Imaging 30: 1615–1619. PMID: 14504831

22. McDermott GM, Chowdhury FU, Scarsbrook AF. Evaluation of noise equivalent count parameters as indicators of adult whole-body FDG-PET image quality. Ann Nucl Med 27: 855–861. doi: 10.1007/s12149-013-0760-2 PMID: 23925895

23. Schaart DR, van Dam HT, Seifert S, Vinke R, Dendooven P, Löhner H, et al. A novel, SiPM-array-based, monolithic scintillator detector for PET. Phys Med Biol 54: 3501–3512. doi: 10.1088/0031-9155/54/11/015 PMID: 19443953

24. Li X, Lockhart C, Lewellen TK, Miyaoka RS. Study of PET Detector Performance with Varying SiPM Parameters and Readout Schemes. IEEE Trans Nucl Sci 58: 590–596. PMID: 22685348

25. Wagadarikar AA, Ivan A, Dolinsky S, McDaniel DL. Sensitivity Improvement of Time-of-Flight (ToF) PET Detector Through Recovery of Compton Scattered Annihilation Photons. IEEE Trans Nucl Sci 61: 121–125.

26. Delso G, Martinez-Möller A, Bundschuh RA, Ladebeck R, Candidus Y, Faul D, et al. Evaluation of the attenuation properties of MR equipment for its use in a whole-body PET/MR scanner. Phys Med Biol 55: 4361–4374. doi: 10.1088/0031-9155/55/15/011 PMID: 20647598

27. Tellmann L, Quick HH, Bockisch A, Herzog H, Beyer T. The effect of MR surface coils on PET quantification in whole-body PET/MR: results from a pseudo-PET/MR phantom study.

28. MacDonald LR, Kohlmyer S, Liu C, Lewellen TK, Kinahan PE. Effects of MR surface coils on PET quantification. Med Phys 38: 2948–2956. PMID: 21815368

29. Paulus DH, Braun H, Aklan B, Quick HH. Simultaneous PET/MR imaging: MR-based attenuation correction of local radiofrequency surface coils. Med Phys 39: 4306–4315. doi: 10.1118/1.4729716 PMID: 22830764

30. Wollenweber SD, Delso G, Deller T, Goldhaber D, Hüllner M, Veit-Haibach P. Characterization of the impact to PET quantification and image quality of an anterior array surface coil for PET/MR imaging. MAGMA 27: 149–159. doi: 10.1007/s10334-013-0388-1 PMID: 23800803

31. Weirich C, Brenner D, Scheins J, Besancon E, Tellmann L, Herzog H, et al. Analysis and correction of count rate reduction during simultaneous MR-PET measurements with the BrainPET scanner. IEEE Trans Med Imaging 31: 1372–1380. doi: 10.1109/TMI.2012.2188903 PMID: 22374353